Automatic Voltage Control (AVC) System under Uncertainty from Wind Power

Qin, Nan; Abildgaard, Hans; Flynn, Damian; Rather, Zakir Hussain; Bak, Claus Leth; Chen, Zhe

Published in:
Proceedings of 19th Power Systems Computation Conference (PSCC)

DOI (link to publication from Publisher):
10.1109/PSCC.2016.7540864

Publication date:
2016

Document Version
Early version, also known as pre-print

Automatic Voltage Control (AVC) System under Uncertainty from Wind Power

Nan Qin and Hans Abildgaard
Energinet.dk
Tonne Kjærsvej 65, Fredericia, DK-7000, Denmark

Damian Flynn and Zakir Hussain Rather
Electricity Research Centre, University College Dublin,
Belfield, Dublin 4, Ireland
Claus Leth Bak and Zhe Chen
Dept. of Energy Technology, Aalborg University
Pontoppidanstræde 101, Aalborg, DK-9220, Denmark

***Abstract*—An automatic voltage control (AVC) system maintains the voltage profile of a power system in an acceptable range and minimizes the operational cost by coordinating the regulation of controllable components. Typically, all of the parameters in the optimization problem are assumed to be certain and constant in the decision making process. However, for high shares of wind power, uncertainty in the decision process due to wind power variability may result in an infeasible AVC solution. This paper proposes a voltage control approach which considers the voltage uncertainty from wind power productions. The proposed method improves the performance and the robustness of a scenario based approach by estimating the potential voltage variations due to fluctuating wind power production, and introduces a voltage margin to protect the decision against uncertainty for each scenario. The effectiveness of the proposed approach is demonstrated on IEEE 39-bus model. Further, Monte Carlo simulation is used to verify the results.**

***Index Terms*—Automatic voltage control, forecast uncertainty, optimization, wind energy.**

I. Introduction

Wind generation met 42% of the demand in the Danish power system in 2015, and is aiming for 50% by 2020 [1]. Consequently, conventional power plants have fewer operating hours and being phased out. The transfer capacities on the interconnections are being increased to maintain transmission security. In addition, the "cable action plan" will partially underground the 400 kV grid and entirely the 150/132 kV overhead lines [2]. A large number of shunt reactors will be placed in the grid to fully compensate the cable capacitance. Consequently, an automatic voltage control (AVC) system is required to minimize the operational cost, i.e. consisting of the power loss, the switching cost of shunts, the cost of tap changes of transformers, while maintaining the system voltage profile within an acceptable band [3]-[5]. Typically, in an AVC system, setpoints for reactive power components, obtained from an optimal reactive power flow (ORPF) algorithm, are dispatched periodically, e.g. every minute. The input parameters for the ORPF algorithms are supplied from a state estimator (SE), which normally takes a minimum of 1 minute to refresh. Therefore, the ORPF decision variables should be valid for at least 1 minute, since changes in the system states are expected to be small and slowly. However, due to an increased share of variable, non-synchronous generation, especially wind power, net system generation variability is increasing and the uncertainty from wind power production, if not taken into consideration, may result in voltage violations in the grid, and consequently lead to redundant/excessive corrective control actions. Therefore, for large-scale wind integrated systems, the uncertainty from wind power production should be directly addressed in the decision making process.

In a typical AVC system, ORPF is based on a realization of the uncertain wind power production to minimize the cost function. If all possible realizations are considered then the problem is a semi-infinite programming (SIP) problem, due to the 'infinite' number of constraints representing power balances for different wind power production levels. The newly formulated problem is solved by approximating the local maximum values of the semi-infinite constraints, which are then solved for the worst case scenario as a normal nonlinear optimization problem. The core issue is to find the binding constraint that is associated with the worst case of the realization, which creates an optimization problem to search for the global optimal point [6]. For the above stated voltage control problem, which is nonlinear and non-convex in nature, to the authors' knowledge, no existing method can efficiently obtain a solution. Therefore, to avoid such complexity, a promising approach is proposed in this paper to effectively control the voltage, while considering wind power uncertainty.

The uncertainty can be modelled as a power density function (PDF) based on historical data. In order to assess different possible situations, the PDF can be discretized to generate scenarios [7], with the power balance associated with each scenario maintained. If a set of control variables is found which satisfies all constraints, then the problem is solved. Normally, the number of scenarios should be large enough to approximate the original PDFs, which results in an intractable problem. This paper improves convergence by relaxing control variables to be slightly different for different scenarios, and then aggregated after the problem is solved. In addition, the paper improves the performance and the robustness of the scenario based approach by including a margin to cover voltage uncertainty arising from wind power production for

each scenario. The decision variables, to a certain degree, guarantee validity over the defined uncertainty range.

The paper is organized as follows. Section II describes the approximate wind power uncertainty model within the load flow calculations, followed by the formulation of the optimization problem for the AVC system in Section III. Section IV introduces the scenario based approach and the relaxation of constraints for better convergence. Section V describes the robustness improvement method based on estimation of the voltage change caused by fluctuating wind power production. Section VI proposes an approach to improve the performance of the scenario based method. Section VII demonstrates the effectiveness of the proposed approach on the test system, followed by concluding remarks in Section VIII.

II. THE UNCERTAINTY MODEL FOR WIND POWER

The existing AVC system under high penetration of wind power is based on a deterministic model, where wind power production is assumed to be certain and unchanging during a dispatching loop. However, wind turbine outputs are not invariant in practice, and the decision variables obtained from such an AVC system may lead to voltage violations, when realized on the grid. It is, therefore, necessary to recognize voltage uncertainty due to the varying wind power production within the decision making process to improve the robustness of the AVC system. Typically, the AVC loop to dispatch setpoints to the reactive power components is less than 5 minutes. In this short term, wind power production may deviate from the observed values used in the ORPF. The deviations can be approximately modelled as a normal distribution profile [8], where the expected value is the measured production value at an AVC loop. A wind power production, $P_{W,i}$, may vary in a range that is described as $\left[\widehat{P_{W,i}} - \Delta P_{W,i},\ \widehat{P_{W,i}} + \Delta P_{W,i}\right]$, where the expected value is $\widehat{P_{W,i}}$ when the measurement is taken from the previous time step, and the deviation magnitudes are $\pm\Delta P_{W,i}$. This interval is centered at $\widehat{P_{W,i}}$, while $\Delta P_{W,i}$ measures the precision. A production realization of a certain wind power production, $P_{W,i}$, can be expressed.

$$P_{W,i} = \widehat{P_{W,i}} + \Delta P_{W,i},\ \Delta P_{W,i} = \theta_i \cdot \widehat{P_{W,i}} \tag{1}$$

where i denotes the busbar index with uncertain wind power generation. $\Delta P_{W,i}$ is a deviation of the wind power production. θ_i is the percentage of the expected value, which complies with the normal distribution, (2).

$$\theta_i \sim Norm(0, \sigma_i) \tag{2}$$

$$\theta_i = \Phi^{-1}(1 - \varepsilon_i),\ 0 < \varepsilon_i \leq 0.5 \tag{3}$$

$$\sigma_i = \sqrt{\frac{\sum(\theta_i)^2}{N_i}} \tag{4}$$

where σ_i is the standard deviation, and N_i is the number of observations of at busbar i. ε_i is defined as the confidence level, that can be used to find the upper and the lower boundaries of uncertainty via (3), where Φ^{-1} is the inverse cumulative normal distribution function. If $\theta_i = 0$, then there is no "protection" against uncertainty, and with $|\theta_i| = \theta_{i,max}$, the entire uncertainty range is covered.

Equations (1)-(4) are a simple approximation of the uncertainty of wind power production, where power production from different wind turbines is assumed to be independent.

III. AVC PROBLEM FORMULATION

The existing ORPF of the AVC system is given in (5)-(9). The objective is to minimize the total real power loss, P_{loss}.

$$\min_{\{x,u\}} P_{loss} \tag{5}$$

subject to

$$\sum_{k=1}^{N} V_i V_k (G_{ik} \cos\delta_{ik} + B_{ik} \sin\delta_{ik}) = P_{l,i} - P_{G,i} - \widehat{P_{W,i}} \tag{6}$$

$$\sum_{k=1}^{N} V_i V_k (G_{ik} \sin\delta_{ik} - B_{ik} \cos\delta_{ik}) = Q_{l,i} - Q_{G,i} - \widehat{Q_{W,i}} \tag{7}$$

$$V_{min} \leq V \leq V_{max} \tag{8}$$

$$u_{min} \leq u \leq u_{max} \tag{9}$$

where the state variables, x, are the voltage magnitudes, V, and the voltage angles, δ. G and B are respectively the grid conductance and susceptance. The control variables, u, are typically transformer tap ratios, shunt susceptances and reactive power output of generators. P_l and Q_l represent the load at a busbar. P_G and Q_G represent the generation excluding uncertain wind power. As long as (5)-(9) is solved, a new power balance is obtained with updated x and u. The equality constraints, (6)-(7), represent the power flow balance, where the expected wind power production, i.e. observed by state estimator $\widehat{P_W}$ and $\widehat{Q_W}$, is normally substituted for the power balancing calculations. However, the actual wind power may be represented as (10) and (11), where the actual reactive power production typically varies according to the active power to maintain a constant power factor, $\cos\emptyset$. The inequality constraint includes the voltage magnitude limits (8) and the regulation capabilities of the controllers (9).

$$P_{W,i} = \widehat{P_{W,i}} + \Delta P_{W,i} \tag{10}$$

$$Q_{W,i} = P_{W,i} \times \tan\emptyset_i \tag{11}$$

IV. SCENARIO BASED APPROACH

A scenario based approach is widely used to solve unit commitment problems [9]. The PDFs of all uncertainties are discretized into samples, with each being the realization of a specific uncertainty. Combinations of samples from different uncertainties compose those scenarios that represent possible realizations associated with different uncertainties. The number of scenarios normally needs to be reduced through scenario reduction techniques in order to solve the problem [7]. A scenario based approach (SBA) can be generally expressed as (12)-(14), [10].

$$\min_{\{x_s, u_{ag}\}} \sum_{s=1}^{N_s} P_s \times f(x_s, u_{ag}) \tag{12}$$

subject to

$$g_s(x_s, u_{ag}) = 0 \tag{13}$$

$$h_s(x_s, u_{ag}) \leq 0 \tag{14}$$

where x_s and u_{ag} are respectively the state and control variables in the scenario s. $f(\cdot)$ is an objective function, e.g. loss minimization. P_s is the probability of each scenario. N_s is the number of scenarios. In (12)-(14), the same control variables, u_{ag}, are obtained for different scenarios after the

problem is solved. The difficulty of applying such an approach is the convergence issue due to the binding constraints (13)-(14). The load flow should converge with the same control variables, u_{ag}, for all involved scenarios, i.e. find x_s for each scenario associated with the common control variables to obtain the power balance for each scenario while satisfying limitations. In order to improve convergence, the problem is realized as defined in (15)-(18), where the control variables for different scenarios, u_s, are constrained within a narrow band $[-\epsilon, +\epsilon]$, as shown in (18). Solving (15)-(18) determines similar control variables that are valid for different load flow conditions formulated from SBA.

$$\min_{\{x_s,u_s\}} \sum_{s=1}^{N_s} P_s \times f(x_s, u_s) \tag{15}$$

subject to

$$g_s(x_s, u_s) = 0 \tag{16}$$

$$h_s(x_s, u_s) \leq 0 \tag{17}$$

$$-\epsilon \leq u_s - u_1 \leq \epsilon \tag{18}$$

Problem (15)-(18) can be solved using a prime dual interior point method (PDIPM). The obtained control variables should be aggregated for dispatching, as there are multiple values for each control variable due to the minor differences introduced by (18). Equation (19) can be applied to aggregate these control variables. As ϵ is a small value, the disturbance introduced by (18)-(19) is minor.

$$u_{ag} = \sum_{s=1}^{N_s} P_s \times u_s \tag{19}$$

V. ROBUSTNESS IMPROVEMENT

If the voltage variation corresponding to fluctuating wind power production can be estimated, then the optimization can incorporate voltage uncertainty as a safety margin to protect decisions against uncertainty. The sensitivities of voltage changes w.r.t. wind power variations are required, which can be obtained by linearization of the load flow equations at the operating point. The impact of uncertainty on the voltage magnitudes can then be estimated.

$$\begin{bmatrix} \Delta P \\ \Delta Q \end{bmatrix} = \begin{bmatrix} J_{P\delta} & J_{PV} \\ J_{Q\delta} & J_{QV} \end{bmatrix} \begin{bmatrix} \Delta\delta \\ \Delta V \end{bmatrix} \tag{20}$$

$$\Delta V_W = \sum_{i=1}^{N_W} \left(S_p \cdot \Delta P_{W,i} - S_Q \cdot \Delta Q_{W,i} \right) \tag{21}$$

$$S_P = (-J_{P\delta} J_{Q\delta}^{-1} J_{QV} + J_{PV})^{-1} \tag{22}$$

$$S_Q = (-J_{Q\delta} J_{P\delta}^{-1} J_{PV} + J_{QV})^{-1} \tag{23}$$

where ΔV_W is a vector representing the voltage changes due to variations of wind power production in a certain scenario. N_W is the number of fluctuating wind power production. S_P and S_Q are sensitivity matrices of voltage changes w.r.t wind power variations, obtained via linearization of the load flow equation (20). The voltage margin of all scenarios, $\Delta V_{W,s}$, to protect the solution against uncertainty can thus be obtained via (20)-(23) for each scenario. The constraint are presented in (24) by considering the voltage margins for all scenarios.

$$V_{min,s} \leq V_{0,s} + \Delta V_{W,s} \leq V_{max,s} \tag{24}$$

where $V_{0,s}$ is a vector representing the operating voltages of busbars for all scenarios. The subscript s denotes the scenario index. $V_{min,s}$ and $V_{max,s}$ are respectively the minimum and the maximum voltage magnitude limits of busbars in all scenarios.

Control actions can also lead to voltage changes that should be taken into account. In the case of nonlinear programming (NLP) technique applied to solve (15)-(18), the impacts on voltage due to control actions are addressed via the provided gradients of the power flow constraints respected to the control variables. Therefore, the voltage variations due to control actions are excluded from (24). In an AVC system, the transformer tap ratios, the susceptance of shunts and the reactive power outputs of the generators are typically defined as control variables. Voltage changes due to the control actions can be expressed as:

$$\frac{dV}{du} = S_v \cdot \frac{dS}{du} \tag{25}$$

where $\frac{dS}{du}$ is the sensitivity of the power change respected to the controller adjustments. S_v is the sensitivity of the voltage change respected to the power change at the nodes, i.e. (22)-(23). The sensitivity matrices of the reactive power changes w.r.t the changes of generator reactive power outputs, dQ_g, and changes of shunt susceptance, dB_{sh}, respectively, are given in (26) and (27).

$$\frac{dQ}{dQ_g} = -1 \tag{26}$$

$$\frac{dQ}{dB_{sh}} = -V^2 \tag{27}$$

The reactive power changes at the sending end, dQ_f and receiving end, dQ_t, respected to the tap ratio changes of the transformers, $d\tau$, respectively, are obtained in (28)-(31).

$$\frac{dQ_f}{d\tau} = \left(V_f \left(\frac{dY_{br}}{d\tau} V_f \right)^* \right) \tag{28}$$

$$\frac{dQ_t}{d\tau} = \left(V_t \left(\frac{dY_{br}}{d\tau} V_t \right)^* \right) \tag{29}$$

$$Y_{br} = \begin{bmatrix} Y_{ff} & Y_{ft} \\ Y_{tf} & Y_{tt} \end{bmatrix} = \begin{bmatrix} \left(y_s + j\frac{b_c}{2} \right) \frac{1}{\tau^2} & -y_s \frac{1}{\tau e^{-j\theta_{shift}}} \\ -y_s \frac{1}{\tau e^{j\theta_{shift}}} & y_s + j\frac{b_c}{2} \end{bmatrix} \tag{30}$$

$$\frac{dY_{br}}{d\tau} = \begin{bmatrix} -\frac{2}{|\tau|} Y_{ff} & -\frac{1}{|\tau|} Y_{ft} \\ -\frac{1}{|\tau|} Y_{tf} & 0 \end{bmatrix} \tag{31}$$

where Y_{br} is the transformer admittance. θ_{shift} is the phase shift angle. V_f and V_t are respectively the sending end and the receiving end voltages. y_s and b_c are respectively the series admittance and the charging susceptances. In the AVC system, for transformers, only the tap ratios are controllable.

VI. PERFORMANCE IMPROVEMENT

The performance of SBA can be improved with fewer scenarios in (15)-(18). The proposed method is described step by step, while the flowchart for the proposed algorithm is shown in Figure 2.

Step 0. ORPF calculation

The classical loss minimization, (5)-(9), is solved using e.g. PDIPM, which provides a feasible starting point for the following steps.

Step 1. Scenario generation

The uncertainties are assumed to be represented as PDFs, which are discretized into several bins, e.g. a continuous PDF is discretized in 7 bins, as shown in Figure 1. The middle value of each bin forms the new variable in the discretized PDF, and the area under the original curve of each bin represents the aggregated probability in the discretized PDF. The aggregated probabilities corresponding to the bins of each PDF are normalized, such that they sum to unity. The bins from different PDFs are combined to represent different realizations, which are so called scenarios. The probability of each scenario is the product of the probabilities corresponding to bins from different PDFs, by assuming that the uncertainties are independent from each other.

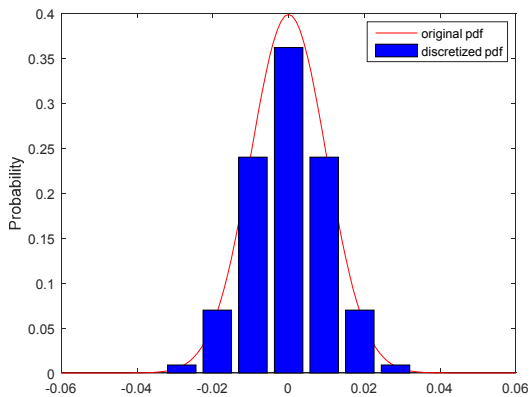

Figure 1. Discretization of a PDF into 7 bins.

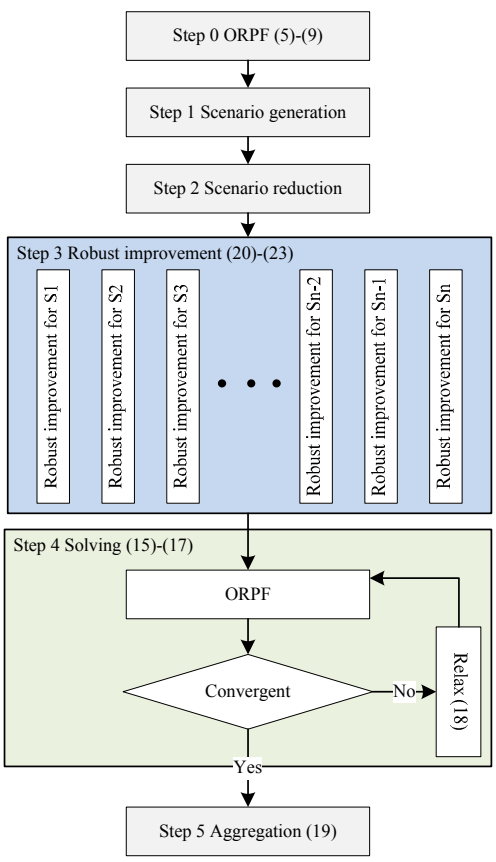

Figure 2. Flowchart of the proposed approach.

Step 2. Scenario reduction

The number of scenarios is reduced to limit the computational burden and improve tractability. After the scenario generation step, the scenario matrix and probability array can be constructed. For the scenario matrix, rows represent the generated scenarios. Entries in the scenario matrix represent the variables of the discretized PDFs. For the probability array, rows represent the scenario indices and the entries are the probabilities of the scenarios. An example is shown in Table 1.

Scenario reduction can be carried out based on evaluations of the Euclidean distance between any two scenarios in the scenario matrix: 1). For each scenario, find the distance to other scenarios, which constructs a distance matrix with entries representing the distance between any two scenarios; 2). Merge the scenario with the lowest probability to the nearest one i.e. with minimum distance; 3). Reconstruct the distance matrix based on the reduced scenario matrix and repeat this process until the desired number of scenarios are obtained. After the scenario reduction step, the probability of some scenarios are extremely low, e.g. lower than $1e-5$. These scenarios normally represent the extreme situations, where the deviations are close to the PDF boundaries. These scenarios can be removed either by setting a higher confidence level in (3), or by directly filtering them out. This step can significantly improve convergence.

Step 3. Robustness improvement for each scenario

Voltage variations due to wind power production are estimated via (20)-(23) for each scenario. The voltage magnitude constraints are therefore updated to include the margins for all scenarios, i.e. (24).

Step 4. Solving problem with relaxation

The reduced scenarios are substituted in the optimization problem (15)-(18). All scenarios are solved simultaneously, where (18) can be tuned to improve convergence.

Step 5. Aggregation of control variables

The control variables should be aggregated via (19) after solving (15)-(18) due to existing minor differences. The aggregated control variables are the final decisions used for the dispatching process.

This approach is used to provide the setpoints for the controllable components in an AVC system taking into account the voltage uncertainty from wind power production. The impacts of wind power variation are assumed to be small in an AVC loop, as the response time of AVC loop is assumed to be shorter than 5 minutes and the wind power production does not change significantly within 5 minutes. In the case that the power deviations are minor, the power balance is maintained by the slack generator without system re-dispatch, while large deviations require activation of Automatic Generation Control (AGC), the active power setpoints of generators, other than the wind turbines, should be updated to meet the power balance constraints, i.e. (16), where the power setpoints are found according to the gain defined in the AGC function. However, comparing to the AGC function, the AVC loop is much faster, and, therefore, the active power setpoints of the generators, other than the wind turbines, may be considered as fixed in each AVC loop.

The voltage margins are found based on the linear estimation of voltage variations respected to the wind power deviations from the expected values, where the wind power deviations are assumed to comply with the normal distribution without any interdependency. In the case of the spatio-temporal correlations among different wind power production being presented, the most severe situation is not able to be captured without considering the dependency. Moreover, the distribution of wind power deviations may be non-parametric. In this case, there is no simple analytical representation to obtain the possible voltage variations due to the fluctuating wind power production. Instead, the spatio-temporal random variable generation techniques, e.g. Normal-to-Anything [11], could be applied to produce the random variables for the Monte Carlo simulations, to determine the largest voltage variation after realization of the found decision variables without considering the uncertainty. The results are updated by reserving the found largest voltage variation. This approach needs Monte Carlo simulations, which is not applicable in the real time system. The assumption made in this paper is considered to be a reasonable approximation to analytically represent wind power deviations for the real time system.

VII. CASE STUDY

The proposed approach is applied to IEEE 39-bus system. In this model, there are 39 busbars and 10 generators, i.e. 6 PV generators are defined as controllers while 3 PQ generators are considered to be wind farms in power factor control mode and the remaining one as a slack generator. The reactive power limits of the slack machine are relaxed, enabling the slack machine to maintain terminal voltage in any situation. There are also 12 tap-able transformers and 2 switchable inductive shunts, which can be used for voltage control. In total, there are 20 control variables, including generator reactive power outputs, transformer tap ratios and shunt susceptances, all adjusted in order to minimize the total power loss, while maintaining voltage magnitudes between 0.95 to 1.05 pu. In this study, all control variables are assumed to be continuous without discretization. The simulation is carried out in Matlab, where the analytical gradients, analytical Hessian matrix, are provided to the built-in PDIPM solver *fmincon* to solve (5)-(9) and (15)-(18). All studies are carried out on a PC with Intel® Core(TM) i7-4600M 2.9 GHz dual processor and 16 GB RAM with a 64-bit system.

A. Optimization considering uncertainty

The 3 generators at buses 30, 31 and 32 are defined as wind farms with uncertain active power production. Assuming: 1). reactive power changes according to the active power to keep the power factor constant; 2). uncertainties of wind power production are independent and with zero covariance; 3). the standard deviation is 1% of their expected values, which corresponds to about $\pm 3.3\%$ of the expected value associated with the confidence level, $\varepsilon = 0.001$.

The SBA discretizes the power production PDFs for the 3 wind farms, where each PDF is discretized to 7 bins, as shown in Figure 1. A total of $7^3 = 343$ scenarios are generated. The scenario reduction technique is applied and the reduced scenarios matrix and probability array are shown in Table 1. As expected, scenarios with high probability represent minor deviations from the expected values. The wind power production is updated for each scenario. In this case, 23 out of 25 scenarios are finally substituted to (15)-(18), as Scenario 23 and 25 in Table 1 have extremely low probabilities that are directly filtered out to improve convergence. The small band for constraining the control variables in (18) is finally set to [-0.003, 0.003]. The robustness improvement method for optimization (RO) reserves the estimated margin of voltage magnitudes to cover voltage uncertainty associated with wind power fluctuations. The margin is calculated using (20)-(23). The RO method applied to improve the SBA performance and robustness, as shown in Figure 2, is named as SRO (scenario based robustness improved optimization).

The power loss in the normal load flow condition without any optimization is 52.98 MW, where the expected wind power production is used for the calculation. In contrast, the results for the different approaches considering a 1% standard deviation of the active power production for the 3 uncertain wind farms are shown in Table 2. ORPF minimizes the power loss by adjusting the setpoints of controllers based on the expected wind power production. The system voltage profile is increased closed to the upper limits, 1.05 pu. The power loss is therefore reduced to 45.96 MW. As there are 3 wind turbines with uncertain production, the introduced voltage variations due to the uncertain wind power production results in voltage violations after the setpoint realizations. In addition, more upper violations than lower violations occur, in Table 2, due to the raised voltage profile. RO, SBA and SRO are applied for improving the feasibilities. The results are assessed by Monte Carlo simulations with 1000 samples. The histograms of the maximum voltage, minimum voltage and power loss for each sample are shown in Figure 3 to 6, respectively. All approaches can improve the likelihood of feasibility, and SRO provides the most promising result.

Table 1. Reduced scenario matrix and probability array of scenarios. Entries of the scenario matrix represent the percentage of expected values for each uncertain wind power production.

Scenario	WG1	WG2	WG3		Probability
1	-0.02	-0.02	-0.02		0.00049
2	-0.02	-0.02	0.03		0.00006
3	-0.02	0.01	0.00		0.00885
4	-0.02	0.02	0.02		0.00039
5	-0.02	0.03	-0.02		0.00006
6	-0.01	-0.01	0.00		0.53305
7	-0.01	0.00	0.03		0.00763
8	-0.01	0.03	0.00		0.00763
9	0.00	0.01	-0.02		0.02489
10	0.00	0.01	0.00		0.38360
11	0.00	0.02	0.02		0.00453
12	0.01	-0.02	0.00		0.00885
13	0.02	-0.02	0.02		0.00039
14	0.02	0.00	0.02		0.00512
15	0.02	0.02	-0.02		0.00039
16	0.02	0.02	0.00		0.00611
17	0.02	0.02	0.03		0.00004
18	0.02	0.03	0.02		0.00004
19	0.03	-0.02	-0.02		0.00006
20	0.03	-0.01	0.00		0.00763
21	0.03	0.00	0.03		0.00007
22	0.03	0.02	0.02		0.00004
23	0.03	0.03	-0.02		0.00000
24	0.03	0.03	0.00		0.00007
25	0.03	0.03	0.03		0.00000

Table 2. Results of 1000 sample Monte Carlo simulations.

Approach	Loss (MW)	No. of upper bound violations	ΔV_{max} (pu.)	No. of lower bound violations	ΔV_{min} (pu.)	Time (sec.)
ORPF	45.96	501	0.005663	1	0.000054	0.19
RO	45.99	276	0.001259	5	0.000382	0.36
SBA	47.46	421	0.001382	0	0	5.71
SRO	46.30	44	0.000261	1	0.000071	4.87

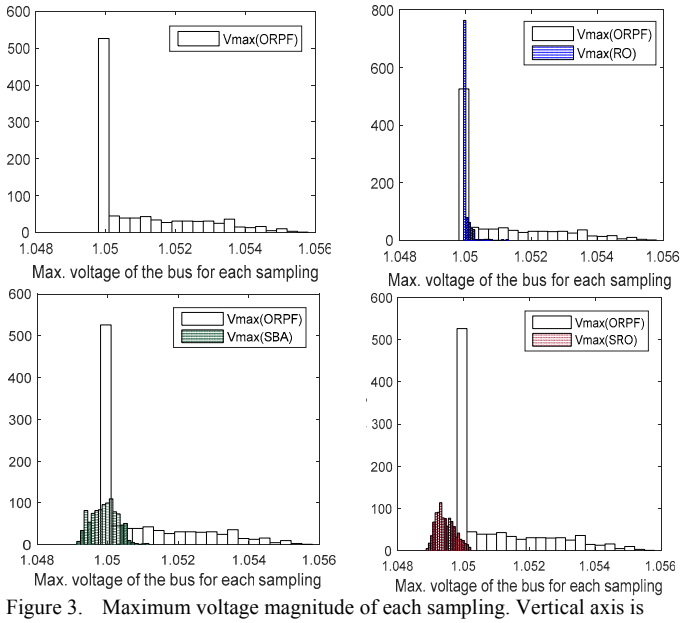

Figure 3. Maximum voltage magnitude of each sampling. Vertical axis is the number of the samples.

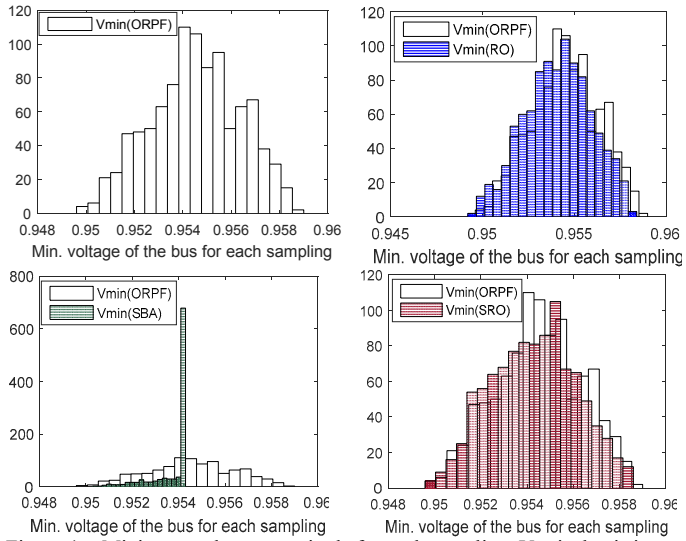

Figure 4. Minimum voltage magnitude for each sampling. Vertical axis is the number of the samples.

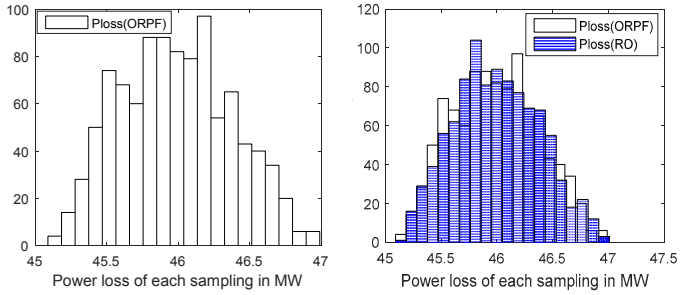

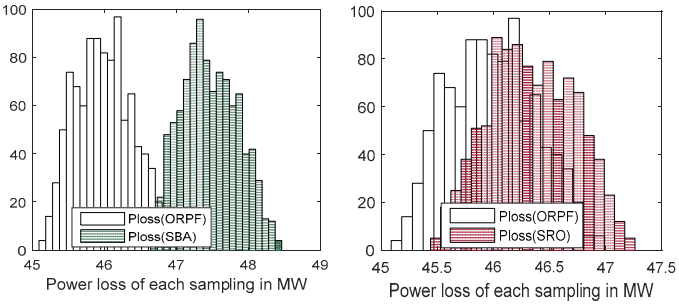

Figure 5. Power loss for each sample. Vertical axis is samples' number.

As shown in Table 2, the voltage violations are generally small in these studies, as assumption (3) constrains the possible variation ranges of the wind power production. Moreover, the reactive power production is assumed to be close to zero to maintain a high power factor, which brings a minor impact on the voltage variations as the active power production of wind turbines vary. The voltage violations are presented in Table 2, after applying different approaches to protect the solutions against the voltage uncertainty caused by the variations in wind power production. Firstly, the extreme scenarios are filtered out if their probabilities are lower than the predefined threshold, i.e. $1e-5$, which is used to greatly improve convergence. In addition, it introduces some risk of voltage violations to reduce the cost. Secondly, the decision variables from different scenarios are aggregated via (19), as the narrow band in (18) introduces differences between the decision variables used for dispatching purposes. Thirdly, the robustness improvement based on the linear estimations that inherently introduce the inaccuracy as wind power production may varies from the expected values. All these issues can degrade the protection effectiveness, i.e. lead to an insufficient voltage margin.

B. *Sensitivity study*

Table 3. Sensitivity study for SBA and SRO approaches, assuming 7 bins ("7B") for each discretized PDF and different number of scenarios ("S").

Cases		Loss (MW)	No. of Upper bound violations	ΔV_{max} (pu.)	No. of lower bound violations	ΔV_{min} (pu.)	Time (sec.)
SBA	7B10S	46.37	335	0.001142	0	0	1.69
	7B20S	46.33	360	0.000858	0	0	5.91
	7B25S	47.46	421	0.001382	0	0	5.11
	7B30S	49.94	106	0.001402	2	0.000168	5.55
SRO	7B5S	46.59	0	0	297	0.003599	1.00
	7B10S	46.24	220	0.000491	0	0	2.14
	7B20S	46.27	74	0.000270	2	0.000408	3.31
	7B25S	46.30	44	0.000261	1	0.000071	4.79

Table 4. Sensitivity study for SBA and SRO approaches, assuming different numbers of bins ("B") for each PDF and 20 scenarios ("20S").

Cases		Loss (MW)	No. of upper bound violations	ΔV_{max} (pu.)	No. of lower bound violations	ΔV_{min} (pu.)	Time (sec.)
SBA	7B20S	46.33	335	0.000963	0	0	5.81
	9B20S	46.14	365	0.001085	2	0.000208	7.76
	11B20S	46.15	388	0.001556	8	0.000472	19.98
	13B20S	46.06	415	0.001880	4	0.000279	81.41
SRO	7B20S	46.27	71	0.000312	2	0.000245	3.32
	9B20S	46.17	304	0.000594	1	0.000259	6.01
	11B20S	46.19	262	0.000567	7	0.000378	21.34
	13B20S	46.07	351	0.000638	12	0.000693	82.13

The number of bins in the discretized PDFs and the number of remaining scenarios after the reduction step have a significant impact on the final results. Two sensitivity studies for the SBA and SRO approaches are carried out, i.e. 1). assuming the PDFs of the 3 uncertainties are discretized in 7 bins, but different number of scenarios remain for optimization; 2). assuming PDFs of 3 uncertainties are discretized in 7, 9, 11 or 13 bins, and 20 scenarios are finally used for optimization.

The results are shown in Table 3 and 4, where SRO provides the best solution. In Table 3, the number of voltage violation cases reduces as more scenarios remain for optimization. In Table 4, the number of voltage violation cases increases as increasing the number of bins while keeping the same number of scenarios for optimizations. It means, as more bins are used to approximate the original PDFs, more remaining scenarios are needed for the optimization. Otherwise, the critical situations are easily lost, as their probabilities are normally low.

C. Discussion

In an AVC system, after dispatching the setpoints to the components, i.e. generators, shunts and tap-change transformers, wind power production may vary, which can lead to voltage violation problems, as shown in Figure 3 and 5 for ORPF cases. Generally, the price for protecting (control) decisions against uncertainty is the higher cost in the objective function, as shown in Table 2 and Figure 5, where the loss calculated from ORPF is smallest.

The RO method estimates the largest possible voltage variation due to uncertain wind power production, then applies a voltage margin in the decision making algorithm. The simulations show that RO can reduce the likelihood of voltage violations, as shown in Table 2 and Figure 3 to 5 for RO cases. As mentioned, the linearization based estimation will not accurately estimate the voltage variations if the deviation is relatively large, and, therefore, there are still many cases with voltage violations. However, the magnitude of the maximum violation is significantly reduced, in the RO case of Figure 3.

The scenario based approach, i.e. SBA, can also to a certain degree protect decisions made against uncertainty. SBA is sensitive to the number of bins introduced and the number of scenarios used in the calculations. SBA typically requires a large number of bins and scenarios to approximate the original distribution curve precisely. However, SBA based on scenario generation/reduction techniques, is incapable of covering all realizations. As shown in Table 3, for the same number of bins for each PDF, a larger number of scenarios leads to better results, i.e. fewer cases with voltage violations. However, if the number of bins is increased while keeping the number of scenarios unchanged, the results become worse, i.e. more voltage violations occur, as shown in Table 4. This is due to the fact that more bins result in more combinations to cover the original PDFs, which requires more scenarios as part of the optimization. The barriers for implementing large numbers of bins and scenarios are the computational time and the convergence issue. The SBA method searches for control variables that comply with all constraints. Large numbers of scenarios can increase the cost of the objective function, or even result in non-convergence. The main difficulty for solving this problem comes from the power flow constraints, i.e. the solver starts from the same initial point to search for those control variables that fulfill all power balance constraints. In the case of two scenarios being significantly different from each other, the solver may fail to find a solution. Equation (18) is thus used to release the constraint, which significantly improves convergence. However, the aggregation carried out by (19) can also bring unexpected errors into the final decisions, in case the constraining band in (18) is relatively large. In this paper, the numerical setting of optimization convergence is set to $1e-4$, and the band in (18) is set between $\pm 3e-3$.

The calculation time for each study is presented in Table 2 to Table 4. The most time consuming task of SBA and SRO is to operate the created scenario matrix for reductions. It can be concluded that as more uncertain variables are included in the problem, the size of scenario matrix will grow larger. The required number of scenarios is therefore greatly increased. Finally, significantly more time is needed for scenario reduction. Parallel computing may be used for scenario reductions, which is out of scope for this paper. In addition, as more scenarios remain for the optimization calculations, more time is generally needed to solve the problem, because more scenarios provide more constraints to the optimization problem. In this study, SRO with 7 bins for each of the 3 PDFs and 25 scenarios takes about 4.79 sec. As the number of bins for PDF discretization is increased to 13, the time consumption is thereby increased to about 82 sec. in Table 4. In general, SRO provides the most promising results, i.e. both seen in Table 3 and 4, which can significantly reduce the number of voltage violation cases and the magnitude of the maximum violation.

VIII. Conclusion

This paper studies a scenario based approach, along with robustness improvement, and proposes a scenario based optimization approach with robustness improvement, SRO, to recognize the uncertainty from wind power production within the decision making process of an AVC system. SRO is a combination of SBA and RO methods. SBA is applied based on scenario generation/reduction techniques. A trade-off is required to ensure a sufficient number of scenarios while remaining tractable. More sophisticated scenario generation/reduction techniques are needed to precisely approximate the original PDFs and to accelerate the calculations for online applications. RO estimates the voltage variations due to uncertainty based on the sensitivity calculations. The sensitivities of the voltage magnitudes respected to active power and reactive power are derived, which is used as a voltage margin to protect decisions against uncertainty from variations in wind power production. SRO combines SBA and RO to reserve a margin for all scenarios. The case studies are illustrated on IEEE 39 bus system. The results for different approaches are assessed using Monte Carlo simulations with 1000 samples, respectively. None of the approaches are capable of guaranteeing 100% protection against wind power variability. However, the proposed SRO method can significantly reduce the risk of voltage violations,

which provides the most promising results. Future studies could be conducted for larger system applications, using parallel computing to consider more scenarios while maintaining reasonable lower computational time. Sophisticated scenario generation/reduction methods could be applied to improve the performance. Different PDFs models for representing the uncertainties could be addressed.

REFERENCES

[1] Energinet.dk, http://energinet.dk/EN/El/Nyheder/Sider/Dansk-vindstroem-slaar-igen-rekord-42-procent.aspx

[2] Energinet.dk, "Cable action plan 132-150 kV," May 2011.

[3] N. Qin, H. Abildgaard, P. Lund *et al*., "Automatic voltage control (AVC) of Danish transmission system – concept design," *Cigré USNC*, Houston, October 2014.

[4] N. Qin, S. Chen, C. Liu, H. Abildgaard, C. L. Bak and Z. Chen, "Multi-period Optimization for Voltage Control System in Transmission Grids," *IEEE GM,* Denver, July 2015.

[5] N. Qin, E.Dmitrova, T. Lund, P. Lund, H. Abildgaard, C. L. Bak and Z. Chen, "Robust fallback Scheme for Danish voltage control system," *PES PowerTech 2015*, Eindhoven, June 2015.

[6] R. Hettich and K. O. Kortanek, "Semi-infinite Programming: Theory, Methods, and Applications," *SIAM*, vol. 35 no.3 pp. 380-429, Jul. 2006.

[7] H. Heitsch and W. Romisch, "Generation of multivariate scenario trees to model stochasticity in power management," in *Power Tech, IEEE Russia*, vol., no., pp.1-7, 27-30 June 2005.

[8] B. Hodge, D. Lew, M. Milligan *et al.*, "Wind power forecasting error distributions: An international comparison," *11th International Workshop on Large-Scale Integration of Wind Power into Power System,* Lisbon, Portugal, 2012.

[9] Q. Wang, Y. Guan and J. Wang, "A Chance-Constrained Two-Stage Stochastic Program for Unit Commitment with Uncertain Wind Power Output," *Power Systems, IEEE Transactions on*, vol.27, no.1, pp.206-215, Feb. 2012.

[10] L. Wu, M. Shahidehpour and T. Li, "Stochastic Security-Constrained Unit Commitment," *Power Systems, IEEE Transactions on*, vol.22, no.2, pp.800-811, May 2007.

[11] M. C. Cario and B. L. Nelson, "Modeling and Generating Random Vectors with Arbitrary Marginal Distributions and Correlation Matrix," *Technical Report*, Dep. Of Industrial Engineering and Management Sciences, Northwestern University, Evanston, Illinois, 1997.